Astron. & Astrophys. 48, 245—252 (1976)

Results of Photoelectric Lunar Occultation Observations Obtained at the Hamburg Observatory during 1969–1973

Chr. de Vegt and U. K. Gehlich
Hamburger Sternwarte

Received December 11, 1975

Summary. During the years 1969 to 1973 photoelectric observations of lunar occultations have been obtained at the Hamburg Observatory with the 60 cm f:15 refractor. A total number of 195 observations, including four occultations of the Pleiades stars, has been recorded, 49 of which are reappearance events. For 11 stars a duplicity is indicated and 6 angular diameter determinations could be obtained.

Key words: lunar occultations — double stars

I. Introduction

Photoelectric observations of lunar occultations were started in April 1969 as a routine program with the 60 cm f:15 refractor of the Hamburg Observatory. A pulse counting photometer with an on-line PDP 8/S small computer for data storing and processing has been used. The photometer head has been provided with a special offset guiding equipment which permits the observation of reappearance events. A detailed description of the photometer, the electronics and the operational modus has been given in (de Vegt *et al.*, 1968, 1970, 1971). During the observation period the photometer was operated with different photomultiplier- and filter combinations which are indicated in column 9 of Table 1. Since November 1971 a RCA 4526V1-tube has been used which has proved to be very satisfactory for this kind of work due to its high quantum efficiency and broad spectral response.

A total number of 195 occultations, 49 of these being reappearance events, have been observed, 11 stars have been found to be doubles, and angular diameters could be determined for 6 late-type stars (de Vegt, 1976).

II. Reduction of Observations

1. Method of Reduction

The occultation event of a single star can be described in general by the usual (monochromatic) Fresnel diffraction pattern $F(\omega)$ of a point source at a straight edge. The natural unit ω is expressed by the actual parameters of interest such as $\omega = \text{arc}\,1''\, v_r \cdot t(2d/\lambda)^{1/2}$ where d denotes the moon's distance from the observer and λ the wavelength of observation. For a detailed discussion see (Dierks and Hunger, 1952; Nather and McCants, 1970).

As actual observations will be obtained with an extended spectral bandpass, the response $S(\lambda)$ of the photoelectric equipment, including the transmission of the telescope optics and atmosphere, together with the stellar energy distribution $I^*(\lambda)$ has to be taken into account. Data for stellar energy distributions have been taken from Lamla (1965) and O'Connell (1973).

For the observed occultation trace $I_s(t_i)$ we have then the relation

$$I_s(t_i) = \delta_1 \int_{\lambda_1}^{\lambda_2} S(\lambda)\, I^*(\lambda)\, F[\text{arc}\,1''v_r(t_i - t_0)\cdot(2d/\lambda)^{1/2}]\, d\lambda + Y_0 \tag{1}$$

where t_i is the time of observation at the i-th data point and the four unknown parameters:

t_0 = time of geometric occultation,
Y_0 = sky background,
δ_1 = scale factor proportional to intensity of star,
v_r = actual velocity at moon's limb (see Section II.2)

which are then obtained by a nonlinear least squares adjustment procedure.

In the case of a double star the corresponding diffraction pattern $I_d(t_i)$ is the linear superposition of two point source patterns; thus we obtain

$$I_d(t_i) = \delta_1 \int_{\lambda_1}^{\lambda_2} S(\lambda) I_1^*(\lambda)\, F[\text{arc}\,1''v_r(t_i - t_{01})\cdot(2d/\lambda)^{1/2}]\, d\lambda + \delta_2 \int_{\lambda_1}^{\lambda_2} S(\lambda) I_2^*(\lambda) F[\text{arc}\,1''v_r(t_i - t_{02})\cdot(2d/\lambda)^{1/2}]\, d\lambda + Y_0 \tag{2}$$

which contains the additional two unknown parameters t_{02} and δ_2. In the case of a previously unresolved double star one has to make the approximation $I_1^*(\lambda) = I_2^*(\lambda) = I^*(\lambda)$, where $I^*(\lambda)$ denotes the stellar

Table 1a: Results of photoelectric occultation observations

Date	DM-No.	SAO-No.	m_v	Sp.	Type	Time[UTC]	σ(T)[ms]	Slope[°]	Remarks	
1	2	3	4	5	6	7		8	9	
					1969					
29. 4.	− 4°3296	138832	6.18	gG9	D	20ʰ07ᵐ27ˢ.627	± 2		§	(1)
19. 6.	16°2010	98717	8.3	Ko	D	21 06 43.413	7	42.8±14.9		(1)
2. 9.	24° 601	76368	9.0	Ao	R	23 30 19.768	3	7.0 2.9		(1)
2. 9.	24° 603	76370	9.0	F8	R	23 45 13.800	200		visual	
4. 9.	27° 858	77521	9.1	A	R	23 18 19.251	3			(1)
5. 9.	27° 888	77625	5.52	gG7	D	00 31 48.200	500		visual	
5. 9.	27° 888	77625	5.52	gG7	R	01 27 56.488	1	− 9.4 2.4	diameter	(1)
5. 9.	28° 917	77637	9.0	B9	R	01 46 14.980	6	3.7 19.1		(1)
5. 9.	28° 920	77645	8.7	B5	R	01 57 51.427	8	21.2 9.2		(1)
30. 9.	23° 516	76155	3.88	B7III	D	02 22 15.300	200		visual	
30. 9.	23° 495	76104	8.3	A5	R	02 27 50.706	9	17.5 27.6		(1)
30. 9.	23° 505	76126	5.45	B7IV	R	02 59 38.195	1			(1)
* 30. 9.	24° 547	76140	4.30	B6V	R	03 23 03.191	1	2.6 6.4	double?	(2)
30. 9.	23° 516	76155	3.88	B7III	R	03 37 40.208	2	− 1.6 19.8		(1)
30. 9.	24° 553	76159	5.76	B8V	R	03 48 56.426	1	9.2 3.0		(1)
20.10.	−15°6143	164868	6.6	Ao	D	17 15 43.519	2	−12.8 5.0		(3)
* 19.12.	19° 403	93062	5.66	AoV	D	21 03 00.957	1	1.2 1.5	μAri,double	(3)
28.12.	10°2153	99138	8.8	F5	R	23 34 03.200	500		visual	
29.12.	10°2160	99153	7.6	F8	R	00 09 30.656	4	9.0 4.9		(3)
29.12	10°2166	118355	3.85	B1Ib	D	02 11 47.970	200		visual	
* 29.12.	10°2166	118355	3.85	B1Ib	R	03 30 01.040	2	−21.4 1.3	ρLeo,double	(3)
					1970					
13. 1.	6° 105	109470	5.92	gG7	D	19 16 11.238	2	− 1.9± 2.6		(3)
13. 1.	6° 107	109474	4.43	K5III	D	19 33 27.066	1	6.4 8.4	diameter	(3)
17. 1.	25° 678	76472	7.5	Ko	D	17 37 29.700	500	0.6 0.3	clock error,10 ms	(3)
17. 1.	25° 682	76500	8.5	F5	D	19 35 20.003	3	− 5.1 0.8	10 ms	(3)
17. 1.	25° 685	76514	7.6	G5	D	21 13 46.418	3	− 0.2 0.5	10 ms	(3)
18. 1.	27° 723	76941	6.48	A7V	D	18 11 41.042	1	5.0 3.6	§§	(3)
* 11. 3.	19° 403	93062	5.66	AoV	D	19 09 04.649	1	0.9 0.4	μAri,double	(3)
11. 3.	19° 405	75531	7.8	G5	D	19 25 22.313	1			(3)
12. 3.	23° 483	76036	8.1	G5	D	19 29 09.807	1		10 ms	(3)
* 13. 3.	26° 731	76682	6.44	dF3	D	21 54 19.882	2		10 ms,ADS 3353B	(3)
* 13. 3.	26° 731	76682	6.44	dF2	D	21 54 24.234	2	1.9 1.2	10 ms,ADS 3353A	(3)
13. 4.	24°1800	79790	8.7	A5	D	20 36 06.953	1	0.4 0.3	10 ms	(6)
* 13. 4.	24°1805	79804	7.5	Go	D	21 28 01.654	3	20.0 4.5	double	(6)
* 13. 4.	24°1805	79804	7.5	Go	D	21 28 01.881	1	5.0 3.3	double	(6)
13. 4.	24°1806	79805	6.7	B8	D	21 40 14.192	1	3.0 0.5		(6)
13. 4.	23°1866	79864	6.39	K1III	D	23 53 07.857	1	− 2.0 1.8		(6)
14. 4.	20°2206	80401	8.6	A5	D	21 11 21.840	1	− 3.1 0.5	10 ms	(3)
14. 4.	20°2207	80405	7.6	F8	D	21 54 29.684	1	2.2 0.3	10 ms	(3)
14. 4.	20°2216	80426	8.1	Ko	D	22 38 21.521	1	0.7 0.4	10 ms	(3)
10. 5.	24°1730	79580	5.94	A2V	D	22 07 25.428	1	− 1.1 1.4		(5)
15. 5.	1°2569	118884	8.3	Ko	D	21 47 32.211	1		10 ms	(3)
16. 5.	− 3°3249	138644	7.8	K2	D	21 28 18.773	1	2.5 0.2	10 ms	(6)
18. 9.	19° 354	93033	7.1	Ko	R	22 13 17.263	3	5.1 28.4		(3)
* 18. 9.	19° 403	93062	5.66	AoV	R	23 43 51.010	3	2.2 1.4	μAri,double	(3)
20. 9.	24° 547	76140	4.30	B6V	D	02 18 04.600	500		visual	
20. 9.	24° 547	76140	4.30	B6V	R	02 41 56.874	500		visual	
22. 9.	27° 806	77295	6.34	Ko	R	00 14 18.910	4	− 0.7± 0.5	10 ms	(3)
* 22. 9.	27°1122	78417	6.42	F5	R	22 45 38.429	1		double?	(3)
23. 9.	26°1264	78476	9.1	Fo	R	00 08 04.689	5	1.4 5.2		(3)
23. 9.	26°1272	78502	8.9	Ko	R	00 46 21.757	4	− 4.1 3.6		(3)
23. 9.	27°1148	78501	8.0	Ko	R	00 57 19.142	1	11.5 6.2		(3)
23. 9.	27°1153	78518	8.9	Ao	R	01 20 23.347	2			(3)
24.10.	15°2091	98691	8.6	G5	R	01 25 28.555	4	− 7.6 46.0		(3)
* 7.11.	−12°6209	164935	7.1	G5	D	17 24 00.068	1		double?	(3)
7.11.	−12°6212	164940	8.8	Ko	D	18 01 44.113	4			(3)
7.11.	−11°5791	164970	8.8	F8	D	19 40 34.983	7	−44.4 13.2		(3)
13.11.	23° 505	76126	5.45	B7IV	D	21 21 49.700	500		visual	
13.11.	23° 547	76140	4.30	B6V	D	21 37 51.500	500		visual	
13.11.	24° 550	76149	8.6	A2	D	21 48 15.700	500		visual §§§	
13.11.	23° 516	76155	3.88	B7III	D	21 54 13.500	500		visual	
* 13.11.	24° 547	76140	4.30	B6V	R	22 49 06.202	1	15.2 6.4		(5)
13.11.	23° 516	76155	3.88	B7III	R	22 59 14.743	1	− 4.4 2.7		(5)
13.11.	24° 553	76159	5.76	B8V	R	23 12 53.388	3	20.8 9.4		(5)
3.12.	−15°6022	164144	8.3	G5	D	18 05 29.322	3	0.3 0.5	10 ms	(4)
23.12.	−14°3739	157998	5.65	gK2	R	04 20 21.887	4	− 7.0 5.1		(4)
31.12.	−15°6042	164591	9.0		D	16 18 38.500	500		visual	
					1971					
2. 1.	− 2°5971	146730	8.7	K2	D	17 06 18.300	500		visual	
2. 1.	− 1°4443	146735	7.1	Go	D	18 01 12.674	1	0.0 0.4	10 ms	(4)
2. 1.	− 1°4450	146756	6.46	gK1	D	18 54 40.976	1	10.0 1.5		(4)
2. 1.	− 1°4451	146761	8.8	F8	D	19 24 57.545	2	− 8.4 3.3	10 ms	(4)
3. 1.	5° 40	109161	8.7	Ko	D	19 03 54.713	3	− 2.0± 0.7	10 ms	(4)
3. 1.	5° 47	109171	9.2	Ko	D	19 31 31.162	5	−18.9 4.0	10 ms	(4)
1. 2.	15° 273	92663	8.2	Ko	D	18 38 12.698	1	3.8 5.4		(4)
3. 2.	24° 546	76137	5.65	B8V	D	19 11 22.965	1	− 0.5 13.9		(4)
4. 3.	27° 771	77177	7.9	F8	D	19 25 37.092	8	−22.4 2.7		(4)
4. 3.	27° 794	77266	7.9	Fo	D	22 55 46.166	4	−12.1 18.8		(4)
5. 3.	26° 870	77322	5.69	B8III	D	00 25 44.155	3	6.0 1.7	ADS 4208A	(4)
6. 3.	24°1627	79309	8.8	K5	D	19 52 06.600	7	4.8 2.6		(4)
* 29. 4.	25°1446	78778	7.2	K2	D	21 51 06.547	2	− 4.0 3.1	double	(6)
* 29. 4.	25°1446	78778	7.2	K2	D	21 51 07.091	1	− 4.0 3.1	double	(6)
30. 4.	23°1780	79607	6.05	K5	D	19 50 15.731	1	25.6 0.8		(6)
30. 4.	23°1790	79619	8.8	A7	D	20 14 38.974	3	−29.0 10.1		(6)
30. 4.	23°1792	79621	8.1	Ko	D	20 24 33.146	1	8.2 5.7		(6)
1. 5.	19°2047	97965	8.5	Ao	D	22 07 47.364	2	11.2 10.5		(6)
1. 5.	19°2049	97971	8.6	A2	D	22 20 11.483	2	21.9 14.3		(6)
3. 5.	10°2112	98964	4.43	K4III	D	20 45 44.991	1	− 4.9 1.0	diameter	(4)
3. 5.	10°2116	118138	7.5	Mo	D	21 55 46.362	2	−17.7 6.9		(6)
2. 9.	−19°5921	163869	7.6	Fo	D	21 20 18.052	1		10 ms	(6)
2. 9.	−19°5928	163887	6.8	F5	D	22 14 25.644	1	− 04 0.9	10 ms	(6)
7. 9.	11° 164	92351	8.9	G5	R	19 58 52.475	5		10 ms	(9)
7. 9.	12° 169	92402	8.9	K2	R	22 29 23.619	3	− 1.9 3.1		(9)
11. 9.	25° 710	76599	7.7	F5	R	00 30 34.051	1	10.7 13.1		(8)
29. 9.	−22°5384	189114	5.96	G8IV	D	18 58 24.824	1	− 1.5 0.3		(9)
6.10.	20° 484	75673	4.6	A2V	R	23 28 59.614	4	5.4 2.9	4 ms;ADS 2257A	(12)
6.10.	21° 357	75671	6.7	A3	R	23 52 55.768	2		4 ms;ADS 2253A	(12)
26.10.	−23°15872	188737	7.6	A2	D	17 27 51.912	1	0.6± 1.5		(6)
26.10.	−23°15870	188736	8.5	Ko	D	17 39 51.624	6	−18.3 8.1		(6)
26.10.	−23°15885	188756	8.9	Fo	D	18 02 36.948	2	− 5.8 3.7	4 ms	(6)
27.10.	−18° 5805	163975	5.91	gKo	D	20 07 59.987	1	7.0 1.8		(9)
29.10.	− 7° 5818	146186	8.5	Ko	D	17 35 31.805	1	0.5 0.2	10 ms	(9)
29.10.	− 7° 5825	146227	8.9	G5	D	19 17 39.623	1	0.0 0.3	10 ms	(9)
29.10.	− 7° 5828	146233	8.9	G5	D	19 41 02.011	1	− 1.3 0.2	10 ms	(9)
29.10.	− 7° 5827	146232	7.1	Go	D	19 53 07.834	1	− 5.4 0.9	5 ms	(9)
29.10.	− 7° 5830	146243	9.1	Go	D	20 46 18.480	2	2.5 0.7	10 ms	(9)
29.10.	− 6° 6052	146247	8.6	Go	D	21 01 39.883	1	− 0.5 0.3	10 ms	(9)
29.10.	− 6° 6060	146264	9.1	Ko	D	21 24 18.455	1	− 3.0 1.3	10 ms	(9)
29.10.	− 7° 5839	146275	8.1	Ko	D	21 48 06.939	2	− 0.3 0.3	10 ms	(9)
30.10.	− 1° 4440	146725	7.8	F8	D	17 07 48.897	1	0.2 0.4	10 ms	(9)
30.10.	− 1° 4446	146749	8.6	K2	D	18 29 46.789	1	− 0.2 0.3	10 ms	(9)
30.10.	− 0° 4520	146744	9.0	K2	D	18 37 56.770	3	1.7 0.7	10 ms	(9)
6.11.	25° 1406	78682	2.99	G8Ib	D	22 23 51.800	500		visual	
6.11.	25° 1406	78682	2.99	G8Ib	R	23 26 10.581	1	− 6.9 4.7	diameter	(9)
24.11.	−15° 5990	164410	9.2	Ko	D	16 55 17.196	3	− 1.8 1.2	10 ms	(9)
24.11.	−15° 5992	164420	9.0	Go	D	17 36 13.445	4	0.9 0.4	10 ms	(9)
29.12.	23° 507	76131	3.69	B6III	D	00 40 29.893	1			(11)
29.12.	23° 505	76126	5.45	B7IV	D	00 42 20.640	1	− 8.2 1.8		(11)
29.12.	23° 516	76155	3.86	B7III	D	01 12 56.272	1	− 2.4 0.5		(11)
* 29.12.	23° 522	76172	4.16	B6IV	D	01 36 47.459	1	1.1 0.2		(11)
29.12.	23° 536	76192	8.1	Ao	D	01 44 48.374	1	8.1 4.1		(11)
* 29.12.	23° 541	76199	2.86	B7III	D	01 48 36.821	1	1.1 0.6	double	(11)
29.12.	23° 553	76216	6.6	Ao	D	02 13 26.501	2	− 5.0 9.9		(11)
29.12.	23° 558	76229	5.09	B8p	D	02 29 12.182	1			(11)
* 29.12.	23° 557	76228	3.62	B8III	D	02 34 47.193	1	− 7.3 0.8	double	(11)
					1972					
* 20. 2.	21° 397	75671	6.7	A3	D	17 41 38.061	2	− 2.1± 4.4	ADS 2253B	(10)
* 20. 2.	21° 397	75671	6.7	A3	D	17 41 39.065	2	− 5.2 4.9	ADS 2253A	(10)
20. 2.	21° 396	75670	8.4	Ao	D	17 56 28.670	3	− 7.6 5.7		(8)
22. 2.	26° 783	76955	6.6	B5	D	19 56 53.762	1	7.1 3.6		(10)
22. 2.	26° 789	76970	7.58	G5IV	D	20 52 25.714	2		2 ms	(10)
17. 3.	15° 251	92588	7.6	Ko	D	19 03 44.433	1	11.2 1.9		(8)
18. 3.	19° 409	75545	8.6	Ko	D	19 47 21.462	2			(9)
18. 3.	20° 458	75558	8.0	Ao	D	20 19 29.799	1		2 ms	(9)
* 19. 3.	23° 507	76131	3.69	B6III	D	19 12 55.572	2	− 9.2 0.5	double	(11)
19. 3.	23° 510	76145	8.1	A3	D	19 24 11.870	1	−22.0 11.3		(8)
19. 3.	23° 517	76158	8.0	Ao	D	19 35 06.224	1	− 9.1 26.6		(8)
* 19. 3.	23° 522	76172	4.16	B6IV	D	19 47 39.927	1	8.2 1.5		(12)
19. 3.	23° 523	76173	7.4	Ao	D	20 03 28.514	1	− 3.5 1.6		(8)
* 19. 3.	23° 541	76199	2.86	B7III	D	20 16 41.072	1	− 3.0 2.9	double?	(11)
19. 3.	23° 540	76200	6.8	B9	D	20 30 55.637	1	− 3.8 1.1		(8)
* 19. 3.	23° 557	76228	3.62	B8III	D	20 56 18.984	1		double	(12)
19. 3.	23° 558	76229	5.09	B8p	D	20 57 39.527	1			(8)
19. 3.	23° 569	76251	6.7	B9	D	21 30 20.561	1	−20.8 3.3		(8)
19. 3.	23° 570	76264	6.8	Ao	D	21 39 28.120	2	29.3 1.9		(8)
20. 3.	25° 734	76760	8.6	Go	D	19 11 09.705	1	8.5 1.6	10 ms	(9)
23. 3.	21°1688	79698	8.8	Ko	D	19 05 41.924	4	1.7 0.9	10 ms	(9)
23. 3.	21°1690	79701	8.9	A2	D	19 32 15.710	5	− 0.5 0.7	10 ms	(9)
24. 3.	17°1914	98061	9.0		D	20 33 25.985	1	1.4 4.6	10 ms	(9)
18. 4.	24°1326	78550	8.9	Fo	D	21 04 49.254	2	−15.6 20.4		(9)
18. 4.	24°1328	78557	6.38	A3V	D	21 23 50.087	1	− 5.7 0.2		(9)
18. 4.	24°1332	78572	6.7	A5	D	21 36 32.197	1	−11.0 0.9	ADS 5270A	(9)
20. 4.	18° 1947	97833	8.3	F5	D	19 51 20.257	4	11.6±11.6		(9)
* 22. 4.	8° 2322	118126	8.8	F8	D	21 35 03.817	3		5 ms,ADS 7652	(9)
* 22. 4.	8° 2322	118126	8.8	F8	D	21 35 05.771	2		5 ms,ADS 7652	(9)
22. 4.	8° 2327	118147	8.4	F2	D	23 18 39.349	1	19.6 4.2	5 ms	(9)
22. 4.	8° 2328	118153	8.9	F2	D	23 33 24.064	2		5 ms	(9)
24. 4.	− 1° 2541	138283	8.6	M?	D	19 51 50.204	1	6.6 1.3	5 ms	(9)
24. 4.	− 1° 2540	138280	7.8	Ko	D	20 01 55.561	1		5 ms	(9)
24. 4.	− 1° 2542	138287	8.9	Fo	D	20 36 57.824	2	23.4 1.5	5 ms	(9)
18. 5.	14° 2025	98348	8.9	Ko	D	21 22 23.961	1	26.9 7.8		(9)
18. 5.	14° 2030	98374	8.9	K2	D	22 28 49.701	1	− 1.9 58.8		(9)
21. 5.	− 0° 2437	138182	8.9	Ko	D	21 18 31.821	4	−25.5 13.4		(9)
22. 8.	−18° 5738	163779	5.10	M2III	D	23 24 22.778	1	− 7.2 1.4	2 ms,diam.	(13)
30. 8.	22° 563	76215	5.44	B8V	R	22 06 02.084	1	11.5 49.8		(11)
30. 8.	23° 563	76244	6.16	B9V	R	22 40 08.317	1	− 5.5 3.5		(12)
1. 9.	24° 1040	77770	8.3	Ko	R	23 50 33.159	6			(9)
2. 9.	24° 1045	77790	7.6	G5	R	00 16 25.283	5	− 4.5 3.0		(9)
17. 9.	−24°15209	187947	8.7	Ao	D	19 41 41.862	7	6.2 2.0	10 ms	(9)
17. 9.	−23°15276	187961	8.4	Ko	D	19 52 42,431	1	− 2.8 1.6	10 ms	(9)
28. 9.	24° 897	77345	9.1	Go	R	22 09 31.144	3	2.0 21.3	10 ms	(9)
29. 9.	24° 940	77485	8.3	G5	R	00 30 43.500	1	0.6 0.3	10 ms	(9)
1.10.	20° 1895	79668	9.2	G5	R	01 04 24.113	7	− 6.6 9.8		(9)
2.10.	17° 1903	98033	7.8	Fo	R	01 52 19.851	1	16.9 7.1		(9)
2.10.	16° 1795	98045	8.7		R	02 13 44.758	2	− 9.1 4.9		(9)
2.10.	16° 1802	98062	7.8	Ao	R	02 45 15.726	1	− 1.2 5.5		(9)
2.10.	17° 1922	98078	9.2		R	03 01 19.407	4	−10.5 6.7		(9)
15.10.	−21° 5540	188610	9.1	Ko	D	18 29 46.660	3	24.4 15.7	3 ms	(9)
18.10.	− 8° 5855	146023	5.4	B8	D	17 08 12.736	1	6.5 2.7		(12)
18.10.	− 8°5857	146038	9.1	K2	D	17 45 12.351	2	13.9± 5.1	10 ms	(9)
18.10.	− 8°5858	146043	9.0	M2	D	18 04 53.362	1	16.0 2.4	4 ms	(9)
18.10.	− 8°5862	146056	7.7	A2	D	18 36 14.027	3	22.2 1.3	6 ms	(9)
18.10.	− 7°5765	146062	6.1	Ko	D	19 21 04.492	1	2.3 4.8	2 ms	(10)
14.11.	− 9°5896	145823	8.9	Ko	D	18 11 46.126	1	26.2 4.7		(9)
14.11.	− 9°5899	145827	9.0	Ko	D	19 15 08.235	3	4.3 4.9		(9)
24.11.	19°1896	97463	6.9	Ao	R	21 51 59.218	4	− 7.5 3.5		(12)
24.11.	19°1911	97537	6.08	B9.5V	R	23 59 18.818	1	13.7 8.6		(11)
					1973					
* 13. 1.	19° 403	93062	5.66	AoV	D	19 06 34.193	2	−12.8 0.7	μAri,2 ms,double	(7)
13. 1.	19° 405	75531	7.8	G5	D	19 27 35.748	2	39.4 5.5	2 ms	(6)
7. 4.	23° 824	76931	8.5	Ko	D	20 46 13.892	1	−11.3 10.2		(14)
7. 4.	24° 745	76957	8.9	F2	D	21 30 15.713	3	−32.6 4.9	2 ms	(14)
7. 4.	24° 750	76964	8.6	Ao	D	22 01 59.973	6	− 1.4 5.1	2 ms	(14)
7. 4.	24° 755	76974	5.41	B2V	D	22 18 38.548	1	−12.2 1.1		(15)
9. 4.	21°1524	79117	8.5	Ao	D	21 15 27.376	2	0.9 2.3	2 ms	(14)
9. 4.	21°1528	79131	6.33	dG7	D	21 31 00.384	1	21.7 1.1		(14)
9. 4.	21°1542	79174	7.8	G5	D	22 47 54.558	2	− 8.3 0.7	2 ms	(14)
* 12. 4.	8°2285	117979	7.1	G5	D	21 54 57.974	1		double?	(14)
12. 4.	8°2289	117997	6.7	Ko	D	23 12 54.119	2	16.2 3.3		(16)
15. 8.	− 3°5539	146412	6.21	G5	R	23 13 56.332	1	5.9 12.9	2 ms	(16)
16. 8.	2°4709	128374	5.30	No	R	23 43 57.218	1	− 0.2 0.1	TX Psc,diam.	(17)
31.12.	2°4709	128374	5.30	No	D	18 14 52.079	10	11.5 1.1	Tx Psc	(17)

Remarks: Observations marked by an asteric are discussed in Section III. In column 9 figures in brackets refer to Table 1b.
§ A correction of −10 seconds to the quoted contact time may be possible.
§§ The contact time may be uncertain because of electronic failure.
§§§ The identification of the star is uncertain.

energy distribution of the unresolved double. From the least squares solution for the six unknowns one then gets the separation of both components in scan-direction: $\varrho'' = (t_{02} - t_{01})\, v_r$ and the intensity ratio δ_1/δ_2 of both components.

The above quoted relations (1) and (2) are only valid in the case of negligible angular diameter ($D_s < 0\overset{''}{.}001$), small telescope apertures ($D_T < 80$ cm) and short integration time scales ($\Delta t \cdot v_r < 5 \cdot 10^{-4}$), where Δt denotes the integration time for each data point.

Table 1b. Photomultiplier and filter combinations. In the cases (13)–(17) special interference filters have been used

(1)	RCA 1P21	
(2)	RCA 1P21 + BG 1	
(3)	EMI 9781B	
(4)	EMI 9781B + GG 18	
(5)	EMI 9781B + BG 1	
(6)	EMI 6256S	
(7)	EMI 6256S + BG 12 + GG 385	
(8)	RCA 4526V1	
(9)	RCA 4526V1 + GG 18	
(10)	RCA 4526V1 + VG 9	
(11)	RCA 4526V1 + BG 12 + GG 15	
(12)	RCA 4526V1 + BG 12	
(13)	RCA 4526V1 + SF1	(λ_0 = 7260 Å, $\Delta\lambda$ = 230 Å)
(14)	RCA 4526V1 + DTGR	(λ_0 = 5380 Å, $\Delta\lambda$ = 700 Å)
(15)	RCA 4526V1 + K 2	(λ_0 = 4300 Å, $\Delta\lambda$ = 500 Å)
(16)	RCA 4526V1 + K 6	(λ_0 = 6650 Å, $\Delta\lambda$ = 500 Å)
(17)	RCA 4526V1 + K 7	(λ_0 = 7100 Å, $\Delta\lambda$ = 500 Å)

The results of the reductions are summarized in Table 1, the main ones being the time of geometric contact and the local slope angle together with their formal mean errors obtained from the least squares solution. The quoted contact times are adjusted to UTC by use of the time-signal from HBG (Pragiens, Switzerland), and a correction of +4 ms has been added to allow for the propagation delay of the HF signal. Observations which are discussed in detail are marked by an asterisk.

2. *Definition and Computation of Local Slope Angles*

If θ_1 denotes the position angle of the moon's velocity vector $\boldsymbol{v}$, θ_2 that, at which the star is occulted, and θ_3 the local slope angle (see Fig. 1), the observed velocity of the limb normal to itself is

$$v_r \equiv R = |\boldsymbol{v}| \cos(\theta_1 - \theta_2 - \theta_3) \tag{3}$$

where the parameter v_r has been obtained from the least squares solution of (1) or (2). The rate R_p published in the occultation predictions assuming a spherical moon is:

$$R_p = |\boldsymbol{v}| \cos(\theta_1 - \theta_2). \tag{4}$$

If we introduce the contact angle ψ, which is given by $\psi = \theta_1 - \theta_2$ (if $\psi < -180°$, one has to add 360° in order to restrict the interval to $-180° \leqq \psi \leqq +180°$), and combine the Eqs. (3) and (4), we get the following ambiguous relation:

$$\theta_3 = \psi \pm \arccos(R \cdot \cos\psi / R_p) \tag{5}$$

where arccos denotes the principal value of the cosine.

According to the convention adopted by Evans (1971) the smaller positive result of the expression (5) has to be assigned to the slope angle if $|R/R_p| > 1$, otherwise the negative result. This definition leads to different directions of the slope according to whether ψ is positive or negative.

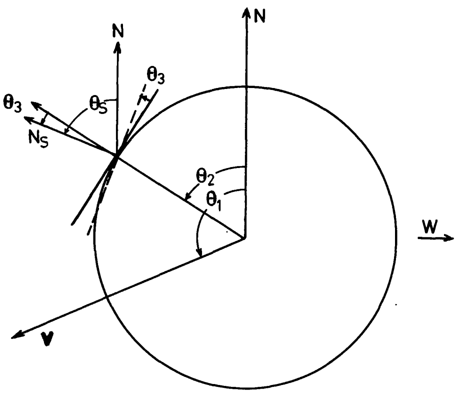

Fig. 1. Geometry of slope angles

We have therefore used a different convention. Consider the normal N_s at the local slope (Fig. 1); if N_s is directed towards a position angle θ_s and $\theta_s > \theta_2$ then the positive solution of (5) is assigned to the local slope angle. In the case of two positive solutions—following Evans—the smaller value is assumed to be the more probable. This definition gives an unambiguous relation between the sign of θ_3 and the direction of the slope at every position angle $\theta_2 + \theta_1$ of the occultation event including reappearances. In accordance with the aforegoing definition the slope angles in Table 1 have been computed from the relation

$$\theta_3 = \begin{cases} \psi - \mathrm{sign}(\psi) \arccos(R \cdot \cos\psi / R_p); & \psi \neq 0 \\ |\arccos(R \cdot \cos\psi / R_p)|; & \psi = 0 . \end{cases} \tag{6}$$

The adopted sign convention for the case $\psi = 0$ is arbitrary. In those cases where the argument of the arccos term has come out >1 due to the observational uncertainty of the involved parameters no slope angles have been derived.

III. Discussion

1. *Limiting Magnitude and Timing Accuracy*

The information, which can be obtained from photoelectric occultation observations depends substantially on the brightness of the occulted star and the amount of scattered moonlight present at the moon's limb. In the following some results will be presented from our observations, obtained at a relatively unfavourable observing site due to its low altitude above sea level (44 m).

About one quarter of all observations have been obtained using a RCA 4526V1 photomultiplier together with a Schott GG 18 filter, yielding a total spectral response according to Fig. 2. In Fig. 3 the amount of scattered moonlight at the dark limb measured through a 10″ diaphragm is plotted versus the moon's illumination, which shows that on normal nights a background level of 100–200 kHz is present, nearly independent of the phase of the moon. This limits the detection of an

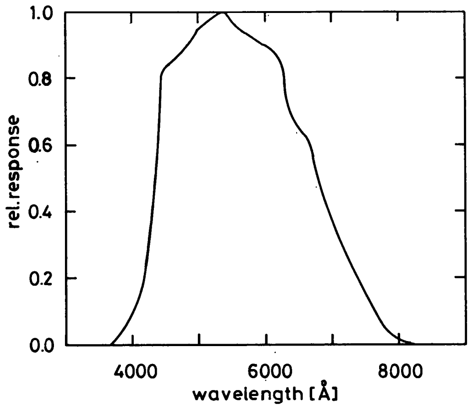

Fig. 2. Photometric response of RCA 4526V1+GG 18, No. (9) in Table 1b

occultation event to stars not fainter than $m_v=9$ with our telescope aperture. For a detailed discussion see (de Vegt *et al.*, 1970). However, although details of the diffraction pattern are not present in such occultation traces, a timing accuracy of better than $0^s.01$ has been regularly obtained. Adopting $v_r \approx 0''.5$/s, this figure would correspond to a formal angular error of about $0''.005$. The present uncertainty in the star positions and local limb profile is $0''.1$–$0''.6$ and $0''.3$ respectively; therefore even a larger timing error would be acceptable. To perform a detailed analysis of the occultation trace arising in connection with the resolution of close doubles or angular diameters, the spectral bandwidth should be restricted to less than 1000 Å, thus decreasing the limiting magnitude to about $m_v=7.5$.

2. *Analysis of Pleiades Occultations*

The occultations of the Pleiades were observed in Hamburg on the following dates: 30.9.1969, 13.11.1970, 29. 12. 1971 and 19. 3. 1972. The observations on 13. 11. 1970 were disturbed by a large amount of scattered moonlight since the occultation occurred only a few hours before full moon.

In the following, details of observations of those stars are presented which are recognized to be double or turned out to have a diffraction pattern deviating significantly from a point source pattern.

BD 24°547 = 19 Tau

The observation on the 30. 9. 1969 is disturbed either by seeing effects or irregularities at the moon limb. Representations of the occultation trace by a single or double star are not satisfactory in both cases. If one adopts the double star solution, a second component would yield $\Delta m \approx 3^m.4$ at a distance of about $0''.01$, position angle $266^\circ.5$. The reappearance observation on the 13. 11. 1970, near full moon, shows no deviation from the diffraction pattern of a point source, although obtained at nearly the same position angle ($270^\circ.7$). Other observations by Berg (1969), Evans (1971) and Bartholdy *et al.* (1975a) are negative or doubtful. Abt *et al.* (1965) found 19 Tau to be a single lined spectroscopic binary with a period of 1313^d. The duplicity from occultation observations must therefore be questioned at present.

BD 23°541 = η Tau

This star was observed twice, on the 29. 12. 1971 and the 19. 3. 1972. On the first date the diffraction pattern obtained is not that of a single star. The result of the analysis yields a double star with $\Delta m = 1^m.58 \pm 0^m.28$ and $\varrho = 0''.0017 \pm 0''.0002$, P.A. $= 114^\circ.1$ (Fig. 4a). The second observation is affected by seeing or irregularities at the moon's limb, but the representation by a double star gives a slightly better result. The computed parameters are: $\Delta m = 1^m.20 \pm 1^m.00$ and $\varrho = 0''.0010 \pm 0''.0004$; P.A. $= 72^\circ.8$ (Fig. 4b). The duplicity is quoted by another observation of Bartholdi *et al.* (1975b).

BD 23°557 = 27 Tau = Atlas

Atlas has been observed twice in Hamburg on 29.12.1971 and 19.3.1972. Since the first measurement was heavily disturbed up to 30 ms before the occultation event, only

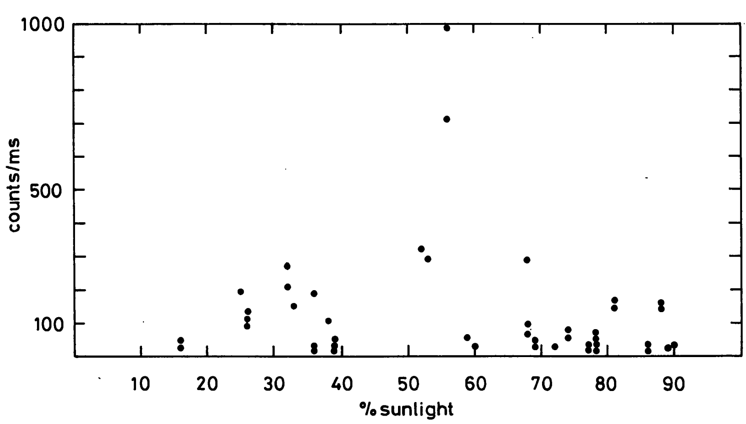

Fig. 3. Intensity of scattered moonlight at the dark limb versus moon's phase

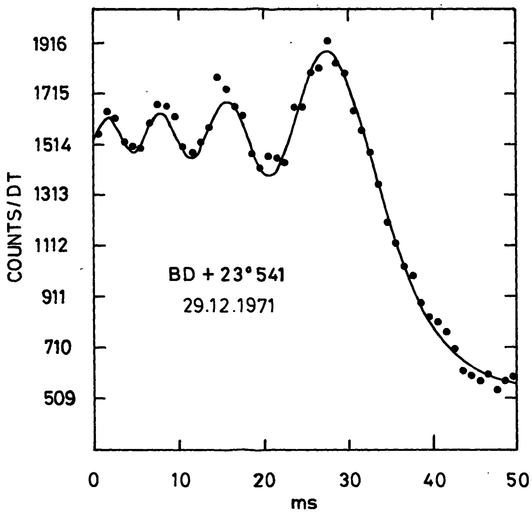

Fig. 4a. Occultation trace of BD+23°541 (double star fit)

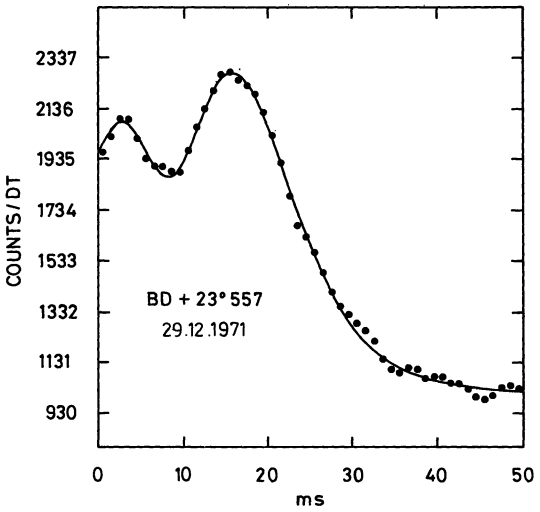

Fig. 5a. Occultation trace of BD+23°557 (double star fit)

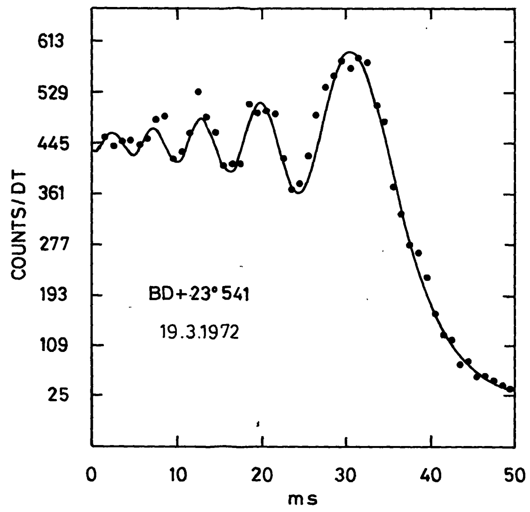

Fig. 4b. Occultation trace of BD+23°541 (double star fit)

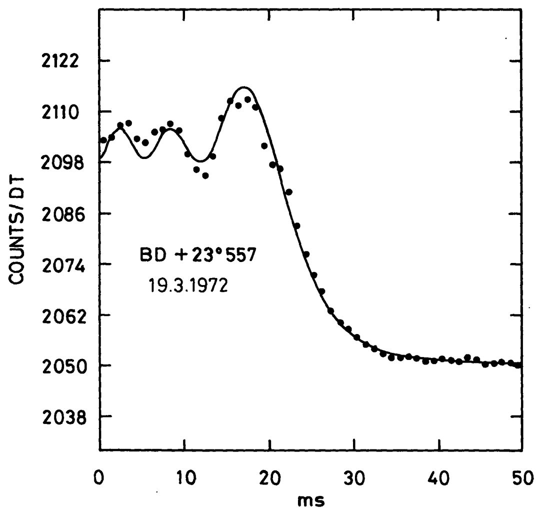

Fig. 5b. Occultation trace of BD+23°557 (double star fit)

a small part of the trace has been analyzed. The model fit results in a double star with $\Delta m = 1^{\rm m}.39 \pm 0^{\rm m}.32$ and $\varrho = 0''.0022 \pm 0''.0005$; P.A. $= 128^\circ.7$ (Fig. 5a). The second observation, although partly affected by seeing effects, results in a double star with $\Delta m = 1^{\rm m}.2 \pm 0^{\rm m}.3$ and $\varrho = 0''.0025 \pm 0''.0004$, P.A. $= 93^\circ.7$ (Fig. 5b). The order of occultation is faint-bright. Fortunately, there is a simultaneous observation of Atlas on the second occultation date by Bartholdi (1975a), yielding $\Delta m = 1^{\rm m}.63$, $\varrho = 0''.0074$, P.A. $= 124°$, and the order of occultation is bright-faint. Combining these data we have computed a true angular separation and position angle of

$$\varrho = 0''.0191 \quad \text{and} \quad \theta = 191^\circ.2 .$$

Adopting a distance of the Pleiades-cluster of 127 pc (Allen, 1973) this angular separation would correspond to a linear distance of 2.43 AU. Whereas a previous observation by Evans (1971) gave no clear indication of duplicity, a further observation, obtained by McGraw *et al.* (1974), clearly indicates the duplicity. Their $\Delta m = 1^{\rm m}.5 \pm 0.1$ is in good agreement with the above quoted results.

BD 23°507 = 17 Tau

The observations were obtained on 19. 3. 1972. The model-fit yielded a slightly better result when the trace was fitted by a double star pattern. The resulting parameters are: $\Delta m = 3^{\rm m}.4 \pm 0^{\rm m}.3$, $\varrho = 0''.010 \pm 0''.001$, P.A. $= 52^\circ.2$. A previous observation by Berg (1969) clearly resolves the double star. Other observations by Evans *et al.* (1971), Eitter and Beavers (1974) show no evidence of duplicity.

BD 23°522 = 23 Tau

The observations of 23 Tau were obtained on 29. 12. 1971 and 19. 3. 1972. Both traces deviate strongly from that of a point source. However it was not possible to

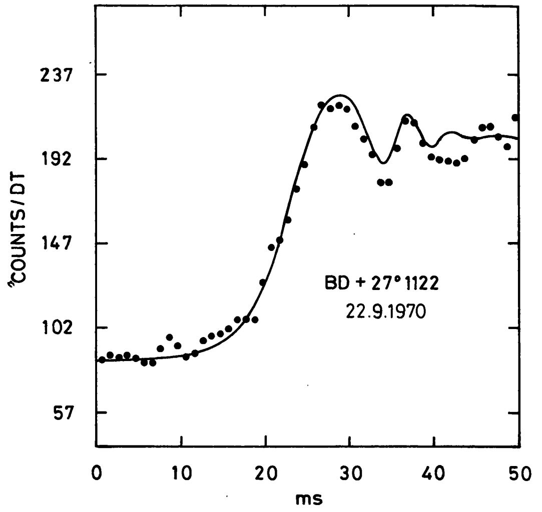

Fig. 6a. Occultation trace of BD+27°1122 (double star fit)

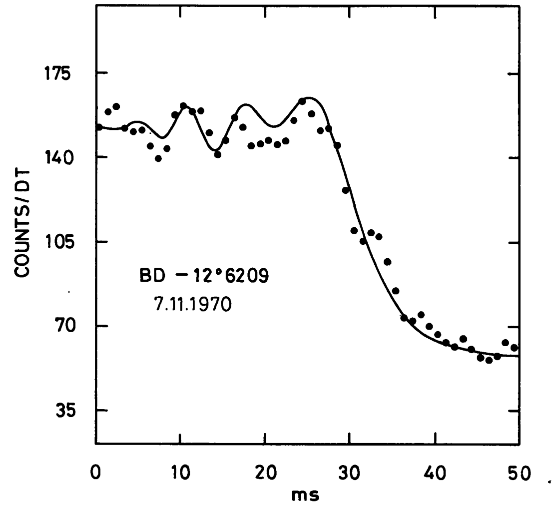

Fig. 6b. Occultation trace of BD−12°6209 (double star fit)

perform a satisfactory double star fit. Additional observations by McGraw *et al.* (1974), Eitter *et al.* (1974), and Bartholdy *et al.* (1975b) do not confirm a duplicity.

3. *Analysis of Other Occultation Observations*

BD 26°731 = ADS 3353

The occultation, observed on 13. 3. 1970, of both components of this visual binary could be measured, the analysis yielding $\Delta m=0^{\rm m}.37\pm0^{\rm m}.10$, $\varrho=2''.117\pm 0''.045$, P.A. $=77^\circ.7$. Since the components have been classified as dF 2 and dF 3 (Hoffleit, 1964) there should be only a small difference in brightness which is confirmed by our result.

BD 10°2166 = ϱ Leo

This star, observed on 29. 12. 1969, is found to be a close double star with $\Delta m=0^{\rm m}.04\pm0^{\rm m}.09$ and $\varrho=0''.0029\pm0''.0001$, P.A. $=276^\circ.5$.

BD 24°1805

The occultation trace, obtained on 13. 4. 1970 is clearly resolved into two components, and the star has not been known to be a double star until now. The analysis of the measurements yields $\Delta m=0^{\rm m}.87\pm0^{\rm m}.11$, $\varrho=0''.074\pm0''.005$, P.A. $=150^\circ.1$.

BD 27°1122

The occultation was observed on 22. 9. 1970. The occultation trace of this star, assumed to be a single one up to now, is affected by seeing effects, but the first maximum is too low for a single star without a measurable diameter ($\phi\leqq0''.0002$). The fit by a double star yields $\Delta m=0^{\rm m}.9\pm0^{\rm m}.7$ and $\varrho=0''.003\pm0''.001$, P.A. $=268^\circ.7$ (Fig. 6a).

BD −12°6209

The noisy observation obtained on 7. 11. 1970 has been fitted by a double star yielding $\Delta m=0^{\rm m}.6\pm0^{\rm m}.3$, $\varrho=0''.004\pm0''.001$, P.A. $=74^\circ.8$ (Fig. 6b). This result must be quoted as doubtful.

BD 25°1446

This star, observed on 29. 4. 1971, is clearly resolved into two components with $\Delta m=1^{\rm m}.15\pm0^{\rm m}.10$, $\varrho=0''.250\pm0''.010$, P.A. $=69^\circ$.

BD 21°397 = ADS 2253

The occultation traces of both components could be observed on 20. 2. 1972, yielding $\Delta m=0^{\rm m}.02\pm0^{\rm m}.11$, $\varrho=0''.352\pm0''.024$, P.A. $=107^\circ.8$.

BD 8°2322 = ADS 7652

The disappearance of both components of this visual binary, observed on 22. 4. 1972, yields $\Delta m=0^{\rm m}.35\pm0^{\rm m}.12$, $\varrho=0''.891\pm0''.026$, P.A. $=107^\circ.2$.

BD 8°2285

This observation, obtained on 12. 4. 1973, could be fitted slightly better by a double star than by a single star. The result is $\Delta m=-0^{\rm m}.01\pm0^{\rm m}.54$, $\varrho=0''.0020\pm 0''.0004$, P.A. $=116^\circ.3$.

BD 19°403 = ADS 2062 = μ Ari

The occultation of ADS 2062 A has been observed four times in different spectral bands under very different sky conditions (see Table 2). The reappearance trace on 18. 9. 1970 has been obtained under very bad weather conditions, but all four observations clearly indicate the duplicity. Three occultation traces show evidence for a third component somewhat fainter than the other two (Fig. 7). The derived parameters have been compiled in Table 2.

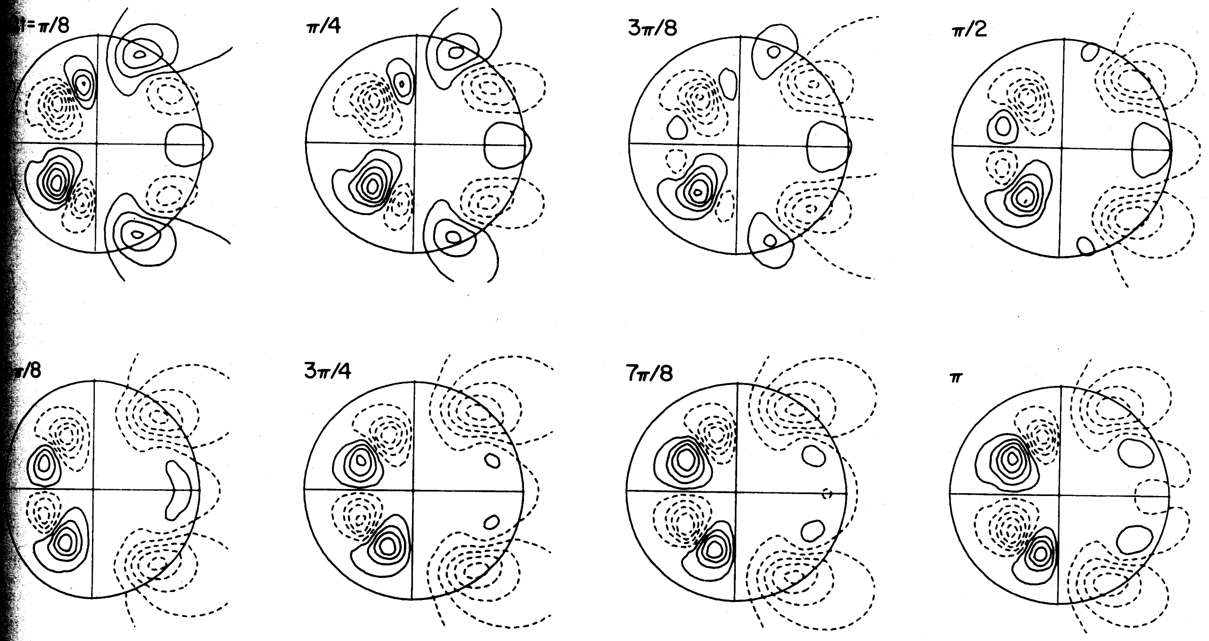

scillatory dipolar magnetic field generated by Model 8, for $\beta_0>0$, $\partial\omega/\partial r>0$. See also legend of Fig. 1

sionless frequency $\Omega=2.85$, and the symmetric upolar) mode has $R_c=28.37$ and $\Omega=3.47$ (both =5, $M=16$).

the preceding section, I have listed the magnetic lds numbers and frequencies in Tables 7 and 8 ome accuracy—not because this accuracy reflects nowledge of the solar dynamo, but in order to ate the convergence, and thus the very existence, various solutions. The frequencies found are of me magnitude, or slightly smaller, as the frequencies -dynamos; a similar value of the (turbulent) tic diffusivity, say 10^8 m^2/s, is therefore necessary pt the models to the real solar cycle. According to (1976) the magnitude of R_β in the Sun should also nparable to R_α, the Reynolds number describing ffect. Thus, the Sun should easily be able to reach tical magnetic Reynolds numbers of Tables 7 and so to generate oscillatory $\boldsymbol{\omega}\times\boldsymbol{j}$-modes.

r $\boldsymbol{\omega}\times\boldsymbol{j}$-dynamo has, however, a few problems: th Models 7 and 8 the *symmetric* mode is excited aller Reynolds numbers, whereas the solar mean s predominantly *antisymmetric*. And as far as rical surfaces of isorotation are concerned, field tion seems to be entirely impossible when the ient a in Eq. (16) is positive, i.e. when the equator s more rapidly than the poles.

nteresting to note that the field generated by l 8 propagates towards the equatorial plane when $/\partial r<0$ (Fig. 4) and towards the poles when $/\partial r>0$ (Fig. 5). Since β_0 should always be positive r, 1976) this means that a solar $\boldsymbol{\omega}\times\boldsymbol{j}$-dynamo adial shear must have an angular velocity which ses with increasing depth. Whether this is a l result of Model 8 or a more general rule for oscillatory $\boldsymbol{\omega}\times\boldsymbol{j}$-dynamos is not yet clear. Since, in contrast to the $\alpha\omega$-dynamos, the analytical treatment in cartesian co-ordinates does not yield oscillatory modes at all (Gubbins, 1974), the confirmation of such a general rule seems to be more difficult.

IV. The Phase of the Poloidal Field

In this section I will return to the concept of a solar $\alpha\omega$-dynamo. In a local cartesian system of co-ordinates the governing equations then essentially describe waves (Parker, 1955; Yoshimura, 1975b). Using Parkers notation, and correcting misprints in his Eqs. (118) $\left[\text{which correctly reads } A_0=-B_0\dfrac{(i\mp 1)\Omega}{k+1}\right]$ and (121), we may write these waves in the form

$$B=B_0\exp\left[\left(\Omega-\frac{k^2}{\mu\sigma}\right)t\right]\exp\left[i(k\xi\pm\Omega t)\right], \tag{18}$$

and

$$A=-B_0\frac{\Omega}{kH}(i\mp 1)\exp\left[\left(\Omega-\frac{k^2}{\mu\sigma}\right)t\right]\exp\left[i(k\xi\pm\Omega t)\right], \tag{19}$$

where k is the wave number, H the shear, $\Omega=|kH\Gamma/2|^{1/2}$ the frequency and Γ the cyclonic strength.

The poloidal field component, corresponding to B_r in the spherical geometry, is $B_\zeta=\partial A/\partial\xi$, i.e.

$$B_\zeta=B_0\frac{\Omega}{H}(1\pm i)\exp\left[\left(\Omega-\frac{k^2}{\mu\sigma}\right)t\right]\exp\left[i(k\xi\pm\Omega t)\right]. \tag{20}$$

The direction of propagation of the wave described by expressions (18) to (20) depends on the product of the shear, H, and cyclonic strength, Γ (or α); the upper signs are valid for $kH\Gamma>0$, and the lower for $kH\Gamma<0$.

de Vegt, Chr., Pansch, E., Schlosser, W. 1970, *Astron. & Astrophys.* **8**, 85
de Vegt, Chr., Pansch, E. 1971, Highlight of Astronomy, IAU XIV, 638
de Vegt, Chr. 1974, *Astron. & Astrophys.* **34**, 457
de Vegt, Chr. 1976, *Astron. & Astrophys.* (in press)
Diercks, H., Hunger, K. 1952, *Z. Astrophys.* **31**, 182
Dunham, D. W., Evans, D. S., Mc Graw, I. T., Sandmann, W. H., Wells, D. C. 1973, *Astron. J.* **78**, 482
Dunham, D. W., Evans, D. S., Vogt, S. S. 1975a, *Astron. J.* **80**, 45
Dunham, D. W., Evans, D. S., Silverberg, E. C., Wiant, J. R. 1975b, *Monthly Notices Roy. Astron. Soc.* **173**, 61P
Eitter, J. J., Beavers, W. I. 1974, *Astrophys. J. Suppl.* **28**, 405
Evans, D. S. 1971, *Astron. J.* **76**, 1107
Hoffleit, D. 1964, Catalogue of Bright Stars, New Haven
Lasker, B. M., Bracker, S. B., Kunkel, N. E. 1973, *Publ. Astron. Soc. Pacific* **85**, 109
Mc Graw, J. T., Dunham, D. W., Evans, D. S., Moffet, Th. J. 1974, *Astron. J.* **79**, 1299
Nather, R. E., Mc Cants, M. M. 1970, *Astron. J.* **75**, 963
Nelson, M. R. 1975, *Astrophys. J.* **198**, 127
Ridgway, S. T., Wells, D. C., Carbon, D. F. 1974, *Astron. J.* **79**, 1079
White, N. M. 1974, *Astron. J.* **79**, 1076

Chr. de Vegt
U. K. Gehlich
Hamburger Sternwarte
Gojenbergsweg 112
D-2050 Hamburg 80
Federal Republic of Germany